

Automated Design of Controlled Diffusion Blades

José M. Sanz
Lewis Research Center
Cleveland, Ohio

(NASA-TM-100251) AUTOMATED DESIGN OF
CONTROLLED DIFFUSION BLADES (NASA) 15 p
Avail: NTIS HC A03/MF A01 CSCL 01A

N88-13304

Unclas

G3/02 0113624

Prepared for the
33rd International Gas Turbine and Aero-Engine Congress and Exposition
sponsored by the American Society of Mechanical Engineers
Amsterdam, The Netherlands, June 5-9, 1988



AUTOMATED DESIGN OF CONTROLLED DIFFUSION BLADES

José M. Sanz
National Aeronautics and Space Administration
Lewis Research Center
Cleveland, Ohio 44135

SUMMARY

A numerical automation procedure has been developed to be used in conjunction with an inverse hodograph method for the design of controlled diffusion blades. With this procedure a cascade of airfoils with a prescribed solidity, inlet Mach number, inlet air flow angle and air flow turning can be produced automatically. The trailing edge thickness of the airfoil, an important quantity in inverse methods, is also prescribed.

The automation procedure consists of a multidimensional Newton iteration in which the objective design conditions are achieved by acting on the hodograph input parameters of the underlying inverse code. The method, although more general in scope, is applied in this paper to the design of axial flow compressor blade sections, and a wide range of examples is presented.

INTRODUCTION

Three dimensional flow analysis codes are increasingly playing a more important role in the design process of axial turbomachinery blading. These codes are generally used to analyze blade configurations that have been designed by two-dimensional methods. The fast computer generation of two-dimensional blade sections with prescribed aerodynamic characteristics still has a central role in the blade design process.

Inverse hodograph codes for the design of controlled diffusion blades have proven to be an excellent source of innovative designs, both in the subsonic and the transonic regime (refs. 1 to 3). One advantage of these methods over direct design methods, aside from the generation of shock-free airfoils, is that the design philosophy can be incorporated into the design process from the start, by imposing a given surface speed distribution which reflects the desired aerodynamic behavior. Also, because the geometry is totally constructed by the method, it can produce body shapes that could hardly be predicted with direct methods (ref. 4). In general, the use of inverse hodograph methods requires expertise on the part of the user; it hardly can be seen as a "black box" method.

Both direct and inverse methods require an iteration procedure to generate a blade section that meets the desired flow characteristics. In the direct design method a specified geometry is modified by interacting with a two-dimensional flow solver until the desired flow conditions are met. In the case of inverse hodograph methods, an airfoil with a prescribed speed distribution is obtained but an iteration process is still necessary to achieve the other geometric and flow requirements.

In this paper an automated procedure is presented that has been developed for use with the Inverse Hodograph Design Code (LINDES) described in reference 5. In this code, three input hodograph design parameters and a prescribed surface pressure distribution control the flow characteristics at the design point. The solidity of the cascade, the inlet Mach number, and the inlet air flow angle are brought to their desired values by modifying the three hodograph design parameters in successive computer runs. The lift imposed by the input pressure distribution determines the air flow turning of the cascade.

The automation procedure described in this paper consists of a multidimensional Newton method in which the objective functions are the cascade solidity, the inlet Mach number, the inlet air flow angle, the air flow turning, and the trailing edge closure or gap conditions. An input speed distribution with three free parameters is used in the automation procedure. The Newton iteration will then use six independent variables to achieve six objective functions.

SYMBOLS

dn_{te}	trailing edge thickness
ds_{te}	streamwise trailing edge gap
M	local Mach number
M_0	hodograph input parameter to control inlet Mach number
M_1	inlet Mach number
Q_M	peak value of input speed distribution
Q_{te}	trailing edge speed
R	hodograph input parameter to control solidity
S_{te}	suction to pressure side arc length ratio
β_1	inlet air angle
$\Delta\beta$	air flow turning
Θ	hodograph input parameter to control inlet air angle
ξ, η	canonical complex characteristic hodograph variables
ρ	density
σ	cascade solidity
ϕ, ψ	potential and stream functions

FIGURES NOMENCLATURE

BET1	inlet air angle, β_1
BET2	exit air angle
DELB	air flow turning, $\Delta\beta$
DNTE	inviscid trailing edge thickness, dn_{te}
DSTE	inviscid streamwise trailing edge gap, ds_{te}
LOSS	loss coefficient
M1	inlet Mach number, M_1
M2	exit Mach number
SOL	solidity, σ
TEV	trailing edge thickness after boundary layer subtraction
THCR	maximum thickness to chord ratio

THE BASE INVERSE HODOGRAPH METHOD

The base inverse design code used for the automation procedure has been described in reference 1, and a users' manual was recently published (ref. 5). The purpose of this section is to review only those aspects of the basic method and design process needed to introduce the input parameters that are to be controlled by the automation procedure. A complete description of the base method is given in the above references and references therein.

The inverse hodograph method constructs an analytical solution for the potential flow equations. The equations for the potential and stream functions φ , ψ , have the hodograph, canonical, complex characteristic form (refs. 1 and 2)

$$\begin{aligned}\varphi_\xi &= \tau_+ \psi_\xi, \\ \varphi_\eta &= \tau_- \psi_\eta,\end{aligned}\tag{1}$$

where

$$\tau_\pm = \pm i \frac{\sqrt{1 - M^2}}{\rho}$$

The computational complex variables ξ and η are defined in a fixed, hodograph-like, domain by means of a solution-dependent conformal transformation. The details of the method have been described in references 1 and 2.

The solution to the system (ref. 1) is expressed in the form

$$\begin{aligned}\varphi(\xi, \eta) &= \text{Re} \left\{ \varphi_1(\xi, \eta) \log(\eta - \eta_1) + \varphi_2(\xi, \eta) \log(\eta - \eta_2) + \varphi_3(\xi, \eta) \right\} \\ \psi(\xi, \eta) &= \text{Re} \left\{ \psi_1(\xi, \eta) \log(\eta - \eta_1) + \psi_2(\xi, \eta) \log(\eta - \eta_2) + \psi_3(\xi, \eta) \right\}\end{aligned}\quad (2)$$

The points η_1 and η_2 correspond to the location of the upstream and downstream singularities, respectively. They are located at the foci (ref. 1) of a fixed ellipse whose boundary corresponds to the subsonic part of the airfoil. The eccentricity of this ellipse determines the distance between these two points, and is prescribed in the code by means of a parameter R , the radius of a circular ring, $1 < |z| < R$, topologically equivalent to the ellipse. By increasing or decreasing the parameter R , the solidity of the cascade σ decreases or increases. The actual value of the solidity is part of the solution, hence the necessity of successive computer runs to adjust to the desired value.

After the single valuedness of the stream function is imposed in equation (2) and the circulation over the airfoil is determined from the input speed distribution, two other arbitrary constants must be specified (ref. 1); this is done by means of two input parameters. These two parameters, M_0 and Θ , control the inlet Mach number, M_1 and inlet air angle β_1 and have to be modified appropriately until the desired values of M_1 and β_1 are achieved.

It was stated in reference 1 that the elliptic transformation introduced there has the property that each of the input parameters R , M_0 , and Θ have a dominant effect over each of the output parameters σ , M_1 , and β_1 , respectively. It is this property of the elliptic mapping that is exploited in the Newton iteration process.

As part of the solution, the body shape is found by using the integral

$$x + iy = \int \frac{e^{i\theta}}{q} (d\varphi + i d\psi/\rho). \quad (3)$$

The residue of this integral, given by the vector

$$dx + i dy, \quad (4)$$

is another output quantity of the design code, it corresponds to the trailing edge opening. The automation procedure adjusts the normal and streamwise components of this vector until the desired trailing edge thickness dn_{te} is obtained, while the streamwise trailing edge gap ds_{te} is forced to vanish. This produces a sharp trailing edge cut normal to the local flow direction and a prescribed trailing edge thickness.

INPUT SPEED DISTRIBUTION

During manual operation of the design code the design goals σ , M_1 , and β_1 are achieved by acting on the input parameters R , M_0 , and Θ previously described. Next, the input pressure distribution is adjusted to obtain the necessary flow turning $\Delta\beta$ and the desired trailing edge gap condition (ref. 1). The flow turning is adjusted by varying the lift and the trailing edge gap by modifying the trailing edge speed and the relative arc length of the blade suction and pressure sides.

In order to be effective, the automation procedure must be able to use a family of pressure distributions defined by as few parameters as possible, but with sufficient versatility to produce the desired geometry. In this work, the speed distribution is defined by piecewise polynomial curves with all its coefficients except three fixed beforehand. For each type of application, different polynomials can be chosen. In particular, Bezier polynomials have proven to be convenient for the present work.

Figure 1 represents a generic speed distribution appropriate for axial compressor blades. In this curve, the trailing edge speed Q_{te} and the arc length S_{te} of either the suction or pressure side are left as free parameters on which the automated procedure can act. A third free parameter Q_M is set as the difference between the peak speed on the suction and pressure sides and by controlling the area under the curve, it has a direct effect on the lift imposed by the speed distribution.

It is worthwhile to note here that other parameters could also be left free, thus increasing the number of independent variables in the Newton iteration. For instance, the slope of the speed distribution at the leading edge has a direct effect on the maximum thickness of the airfoil, and could, conceivably, be added as a new free parameter. But, as stated earlier, the six free design parameters previously described have the important property that each has a dominant effect on one of the design objectives with only a secondary effect on the others.

The new form of definition of the speed distribution, which is essential to the automation procedure, has the additional advantage of making the design process less sensitive to spurious fluctuations in the speed distribution than when it was defined by a cubic spline, as it was previously done on the basic code. Besides, this new mode of defining the speed distribution does not seem to impose any limitation over the possibilities of the underlying code. In fact, because of the capability of making local changes in the areas needed, it promises to enhance these possibilities.

AUTOMATION

Consider the solution to the flow equations, generated by each cycle of the inverse code, as a vector valued function

$$\bar{y} = F(\bar{x}) , \quad (5)$$

where

$$\bar{x} = (R, M_0, \theta, Q_M, Q_{te}, S_{te}) \quad (6)$$

is the vector formed with $N = 6$ input parameters and

$$\bar{y}(\sigma, M_1, \beta_1, \Delta\beta, dn_{te}, ds_{te}) \quad (7)$$

is the vector of output conditions. The objective function for the automation procedure is the vector

$$\bar{y}_0 = (\sigma, M_1, \beta_1, \Delta\beta, dn_{te}, ds_{te})_0 \quad (8)$$

of specified output conditions.

A Newton iteration is established to solve the vector equation

$$\bar{F}(\bar{x}) - \bar{y}_0 = 0, \quad (9)$$

by means of the relation

$$\bar{x}_{n+1} = \bar{x}_n - J^{-1}(\bar{x}_n)(\bar{y}_n - \bar{y}_0), \quad (10)$$

where J is the Jacobian matrix

$$J = \left(\frac{\partial F_i}{\partial x_j} \right) \quad (11)$$

The numerical evaluation of the Jacobian matrix J requires $N + 1$ cycles, one to calculate the starting point and N more, in which all but one of the independent variables are frozen, to compute the partial derivatives in J . Once the Jacobian matrix has been evaluated, it can be inverted and the new input vector \bar{x}_{n+1} is calculated. The process can then be repeated until a given tolerance

$$\text{Tol} = \max |(\bar{y} - \bar{y}_0)_i|, i = 1, N \quad (12)$$

is achieved.

Each iteration step consists of $N + 1$ cycles and yields a second order accurate method. We have found that faster convergence can be obtained by freezing the Jacobian J after the first $N + 1$ cycles have been performed. Although, in this case, the method is then first order accurate, only one cycle is required per iteration step. In either case, some relaxation is added for stability purposes.

The method converges well, about forty cycles are enough to bring the tolerance, 12, below a value of 10^{-3} . In subsonic blade design the procedure is robust and, provided that a judicious choice is made, it will converge to the desired solution even from a relatively distant initial guess.

EXAMPLES

In this section, several examples are presented which have been developed to test the automation procedure. All the examples presented use the same input speed distribution shown in figure 1. As stated earlier, this speed distribution is defined with only three free parameters, Q_{te} , S_{te} , and Q_M , on which the automation can act. The automation will search within this three-parameters family until a speed distribution is found that achieves the objective function. In so doing, the speed distribution shape will change according to the changes imposed on the parameters Q_{te} , S_{te} , and Q_M by the automated procedure.

One important point that the examples show is that starting from the same initial guess of speed distribution a broad range of airfoils can be obtained. A flat top speed distribution has been chosen, which is representative of a design philosophy. Accelerated profiles, for instance, could equally have been chosen and would result in different blade shapes.

As a first example, a stator blade for a low speed fan is chosen. Four sections are designed, all with an inlet Mach number of 0.3 and inlet air angles of 45° , 40° , 35° , and 30° from hub to tip. The four sections, radially equidistant, have solidities varying from 2 at the hub to 1 at the tip. In all sections, the flow is requested to turn to the axial direction.

The same initial guess is used for all sections, and an inviscid trailing edge thickness of 3 percent is imposed in all of them. Figures 2(a) to 5(a) show the inviscid airfoil and output surface Mach number distribution at the design point. Figures 2(b) to 5(b) present the cascade plane with the body shape after the boundary layer has been subtracted.

The next example (figs. 6 to 9) consists of a higher speed blade, inlet Mach number of 0.5, and with the same air inlet angles, flow turning and solidities as the previous case. All the objectives were achieved, but the hub section presented an excessive amount of diffusion when a trailing edge thickness of 3 percent was specified. This section was then redesigned, imposing an inviscid trailing edge thickness of 3.5 percent.

Finally, a transonic, shock-free, tip section is designed with the same flow conditions as the tip sections in the two previous cases, but with an inlet Mach number of 0.7 (fig. 10). Although the design is achieved, it required an initial guess closer to the design point. The parameter M_0 has to be chosen well under the value that produces the objective design, in order to obtain first a subsonic blade of approximately the same solidity, inlet air angle and flow turning. The shock-free design problem is intrinsically different from the subsonic design and special care has to be exercised to produce a relevant case. Although the method solves a mathematically well posed problem, see reference 1 and references therein, there is no guarantee that every given pressure distribution will produce a physically meaningful shock-free solution, hence the necessity of starting from a reasonable guess.

CONCLUSION

In this paper, the automated design of controlled diffusion blades is proven to be feasible. For this purpose, an automation procedure has been developed for the design of axial turbomachinery blading to be used in conjunction with an inverse hodograph design code. With this automated design method, the inlet Mach number, inlet air flow angle, air flow turning, solidity and trailing edge thickness of a cascade of airfoils are prescribed.

Applications to axial compressor stator blade design are presented. Two subsonic blades, each composed of four sections, and one transonic blade section are presented. All cases are produced with a single input speed distribution, defined by three free parameters, on which the automation procedure acts to yield the different blade sections.

REFERENCES

1. Sanz, J.M., "Design of Supercritical Cascades With High Solidity," AIAA Journal, Vol. 21, No. 9, Sept. 1983, pp. 1289-1293.
2. Bauer, F., Garabedian, P., and Korn, D., Supercritical Wing Sections III, Springer-Verlag, New York, 1977.
3. Sanz, J.M., "Improved Design of Subcritical and Supercritical Cascades Using Complex Characteristics and Boundary-Layer Correction," AIAA Journal, Vol. 22, No. 7, July 1984, pp. 950-956.
4. Sanz, J.M., et al., "Design and Performance of a Fixed, Nonaccelerating Guide Vane Cascade that Operates Over an Inlet Flow Angle Range of 60° ," Journal of Engineering for Gas Turbines and Power, Vol. 107, No. 2, Apr. 1985, pp. 477-484.
5. Sanz, J.M., "Lewis Inverse Design Code (LINDES) - Users Manual," NASA TP-2676, 1987.

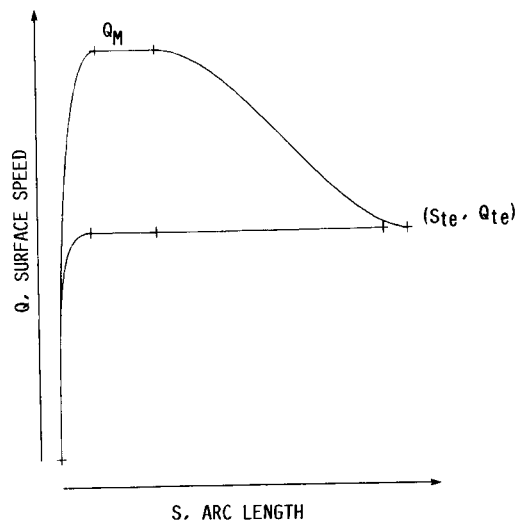


FIGURE 1. - GENERIC SURFACE SPEED DISTRIBUTION.

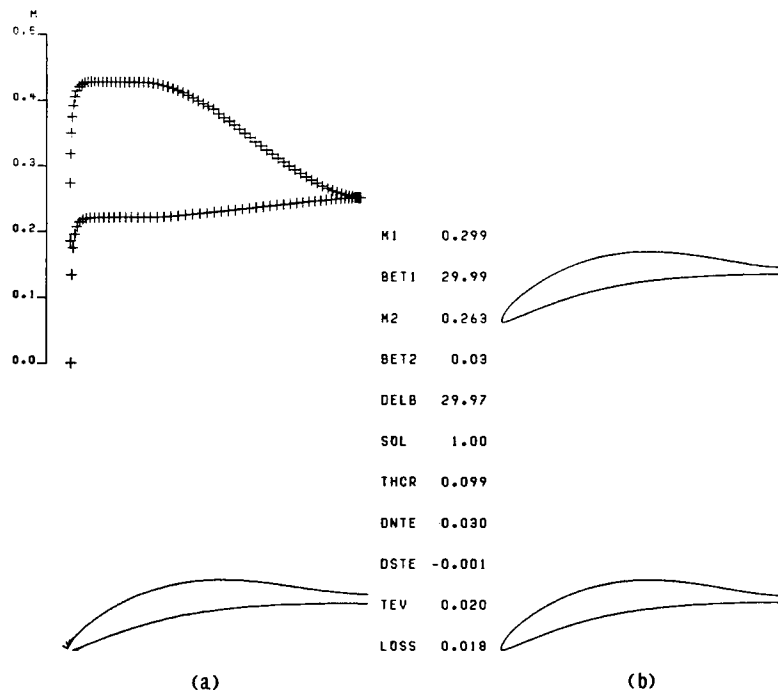


FIGURE 2. - LOW SPEED STATOR TIP SECTION.

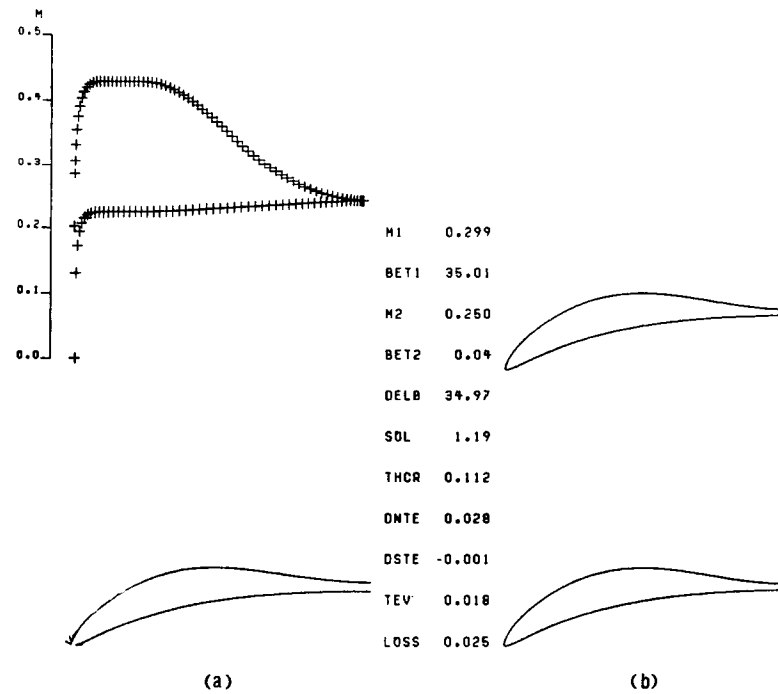


FIGURE 3. - LOW SPEED STATOR MID-TIP SECTION.

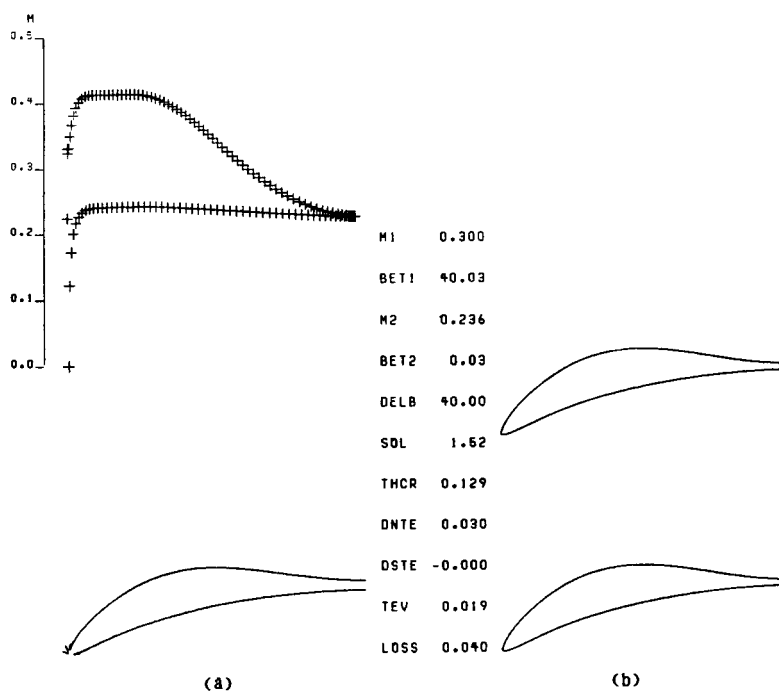


FIGURE 4. - LOW SPEED STATOR MID-HUB SECTION.

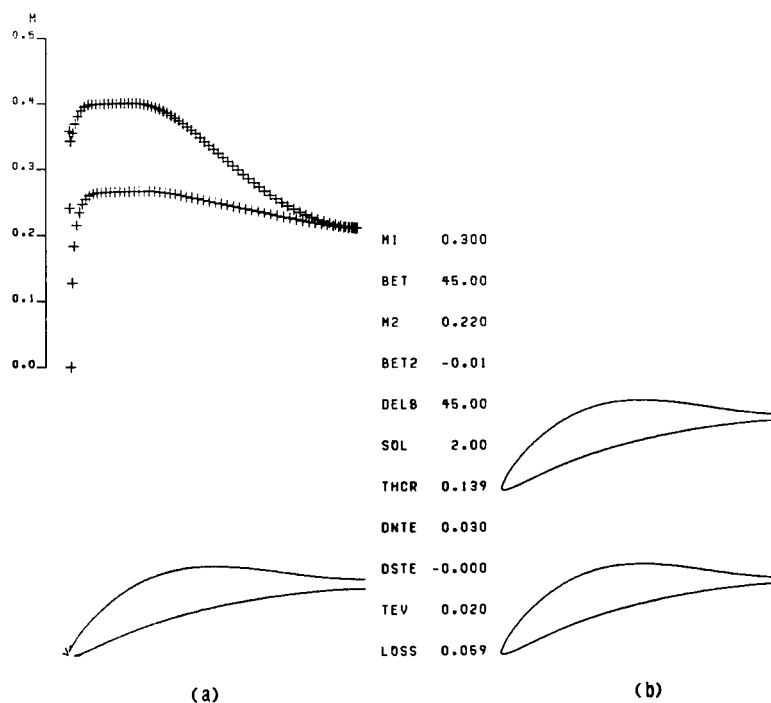


FIGURE 5. - LOW SPEED STATOR HUB SECTION.

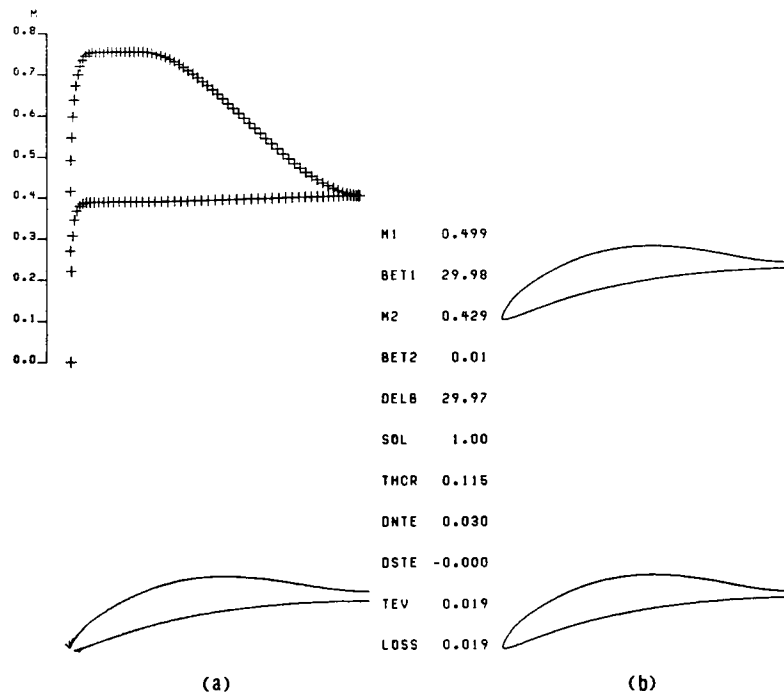


FIGURE 6. - MID SPEED STATOR TIP SECTION.

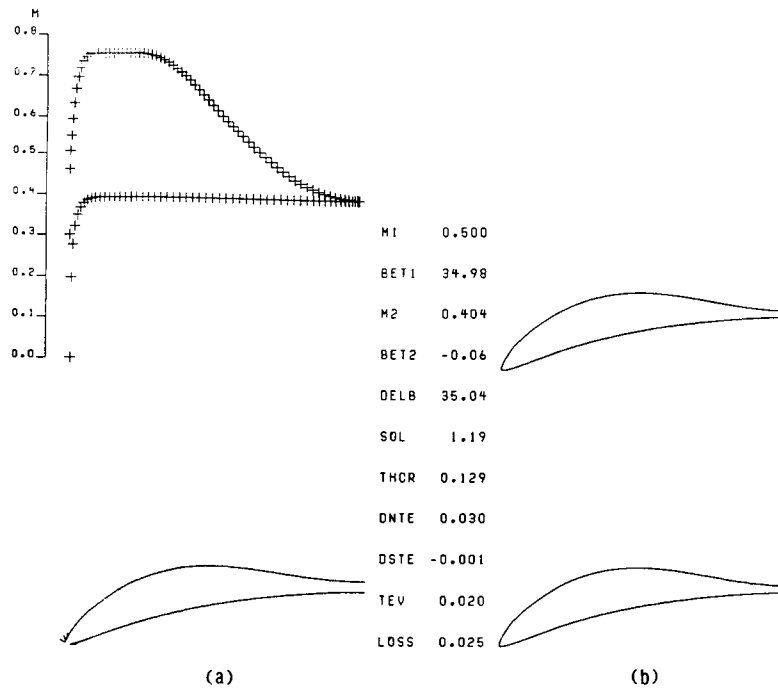


FIGURE 7. - MID SPEED STATOR MID-TIP SECTION.

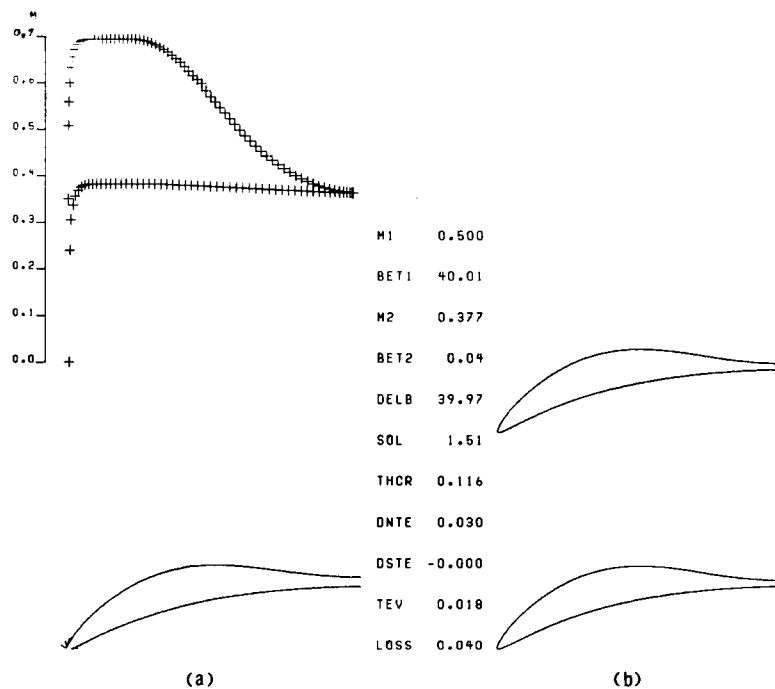


FIGURE 8. - MID SPEED STATOR MID-HUB SECTION.

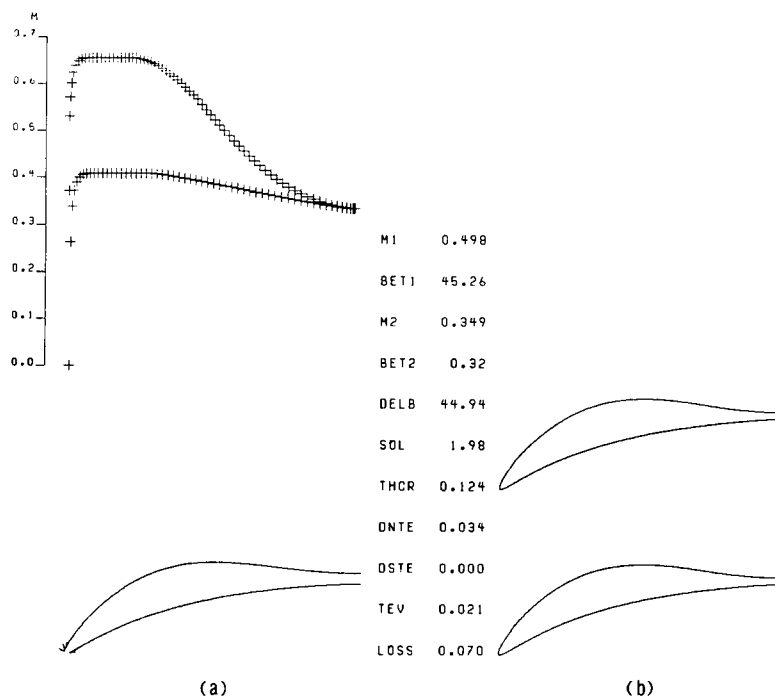


FIGURE 9. - MID SPEED STATOR HUB SECTION.

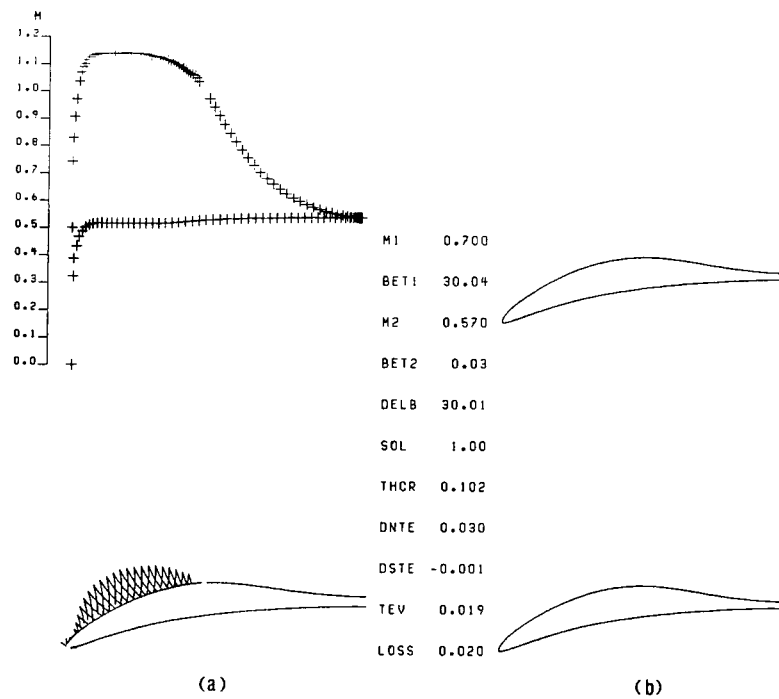


FIGURE 10. - TRANSONIC STATOR SECTION.

1. Report No. NASA TM-100251		2. Government Accession No.		3. Recipient's Catalog No.	
4. Title and Subtitle Automated Design of Controlled Diffusion Blades				5. Report Date	
				6. Performing Organization Code	
7. Author(s) José M. Sanz				8. Performing Organization Report No. E-3877	
				10. Work Unit No. 505-63-21	
9. Performing Organization Name and Address National Aeronautics and Space Administration Lewis Research Center Cleveland, Ohio 44135-3191				11. Contract or Grant No.	
				13. Type of Report and Period Covered Technical Memorandum	
12. Sponsoring Agency Name and Address National Aeronautics and Space Administration Washington, D.C. 20546-0001				14. Sponsoring Agency Code	
15. Supplementary Notes Prepared for the 33rd International Gas Turbine and Aero-Engine Congress and Exposition sponsored by the American Society of Mechanical Engineers, Amsterdam, The Netherlands, June 5-9, 1988.					
16. Abstract A numerical automation procedure has been developed to be used in conjunction with an inverse hodograph method for the design of controlled diffusion blades. With this procedure a cascade of airfoils with a prescribed solidity, inlet Mach number, inlet air flow angle and air flow turning can be produced automatically. The trailing edge thickness of the airfoil, an important quantity in inverse methods, is also prescribed. The automation procedure consists of a multi-dimensional Newton iteration in which the objective design conditions are achieved by acting on the hodograph input parameters of the underlying inverse code. The method, although more general in scope, is applied in this paper to the design of axial flow compressor blade sections, and a wide range of examples is presented.					
17. Key Words (Suggested by Author(s)) Design turbomachinery; Compressors; Cascades; Automation; Inverse design			18. Distribution Statement Unclassified - Unlimited Subject Category 02		
19. Security Classif. (of this report) Unclassified		20. Security Classif. (of this page) Unclassified		22. Price* A02	
				21. No of pages 14	